AAPS PharmSciTech (2025) 26:225
https://doi.org/10.1208/s12249-025-03217-1

RESEARCH ARTICLE

Effects of Roller Compaction on Dissolution of Granules and Tablets Captured in the Development of Two Real Pharmaceutical Formulations

Nikita Marinko[1,3] · Stephanie Michelle Medrano[1,2] · Tomáš Krpelan[1] · Zuzana Chayka[1] · Kateřina Budková[1] · Vít Zvoníček[3] · Petr Zámostný[1]

Received: 24 April 2025 / Accepted: 7 August 2025 / Published online: 3 September 2025

Abstract

Roller compaction is often utilized as the first step to improve flow properties and homogeneity of pharmaceutical mixtures. Since the dry granulation process is less complicated than its counterparts in the industry, it is possible to perform screening experiments readily to investigate granulate quality for further operations. In this study, the aim of the investigation focused on the effect of roller compaction on the dissolution of granules and tablets of two pharmaceutical formulations that contain APIs of different biopharmaceutical classification. This study underscores the benefits of granule dissolution testing as a crucial early-stage technique for optimizing granulate quality and facilitating progression through formulation manufacturing operations. For active pharmaceutical ingredients characterized by poor dissolution properties, this approach provides valuable insights during the initial development phases. By integrating granule dissolution testing into the development process, product manufacturability can be enhanced and optimal product performance can be ensured.

Keywords Disintegration kinetics · Dissolution behavior · Dissolution rate · Dry granulation · Flow-through cell · Granule dissolution · Granule properties · Paddle dissolution · Porosity · Process engineering · Process parameters · Poller compaction · Tablet dissolution · USP2 dissolution · USP4 dissolution

Introduction

Pharmaceutical formulation development relies heavily on granulation techniques to enhance the physicochemical properties of raw materials, aiding their processing and performance in final dosage forms. Among these, roller compaction (RC), a dry granulation method, maintains significant importance for processing heat- and moisture-sensitive active pharmaceutical ingredients (APIs) by preserving their stability. RC involves densifying powders into ribbons under high pressure, followed by milling these ribbons into granules. The operation of dry granulation also leverages scalability, cost and time efficiency, and aligns well with the continuous manufacturing paradigm. Despite its advantages, RC presents challenges, including granule hardening and porosity reduction, which may compromise the final product quality [1–9].

The relationship between granule properties and tablet performance has been extensively explored, with a clear understanding that attributes such as granule porosity, size, and hardness play critical roles in determining the mechanical strength and dissolution performance of the final dosage form. The process parameters of RC induce these structural and mechanical granule characteristics [2, 6, 10–12]. High compaction pressures often yield dense and poorly disintegrating granules with reduced porosity, impeding water penetration and API release during dissolution. This phenomenon is further exacerbated by granule hardening, a factor that limits the fragmentation mechanism during tableting,

✉ Nikita Marinko
nikita.marinko@zentiva.com

✉ Petr Zámostný
petr.zamostny@vscht.cz

1 Department of Organic Technology, Faculty of Chemical Technology, University of Chemistry and Technology, Technická 5, 166 28, Prague, Czech Republic

2 University of Applied Sciences and Arts Northwestern Switzerland, School of Life Sciences, Hofackerstrasse 30, 4132 Muttenz, Switzerland

3 Zentiva k.s., U Kabelovny 130, 102 00, Prague, Czech Republic

which compromises tablet tensile strength. Additionally, the occurrence of large granule sizes, often a byproduct of high roller speeds or excessive compaction force, further restricts dissolution due to a reduction in the surface area available for drug release [1, 5, 13–18]. When this occurs in the granules, it often requires redesigning the parameters of the process or additional modifications to achieve the desired dissolution profile, such as fines recycling or post-compaction treatments, adding complexity to the manufacturing process [2, 19–22]. Therefore, the dissolution behaviour of granules is affected by mechanical factors, mainly compaction pressure, but also by formulation composition, granule morphology and fines content. These factors necessitate a more detailed investigation into how studying intermediate granules can serve as an early indicator of formulation success. Matji et al. (2019) demonstrated that increased compaction pressure during tableting of RC granules significantly delayed disintegration and reduced the quantity of early drug release (5 min) in high-drug-load ibuprofen tablets. These effects were directly linked to reductions in granule and tablet porosity, as quantified by mercury intrusion porosimetry [23]. The impact of excipient selection is equally evident; Chang et al. (2008) observed that lactose-based RC granules formed hydrophobic pellicles under accelerated stability testing, impeding dissolution, whereas mannitol-based counterparts preserved rapid-release characteristics, underscoring the importance of matrix hydration and solid-state stability in dissolution performance [24]. Inghelbrecht and Remon (1998) investigated dry granulation of microcrystalline cellulose and ibuprofen blends, showing that while high ibuprofen levels improved tablet mechanical strength through fragmentation, they also impaired granule quality. The study highlighted that the interaction between deformable and fragmenting excipients introduces complex behaviour in RC, with MCC influencing dissolution more than particle size [25]. While Dular Vovko et al. (2022) conducted a comprehensive multivariate analysis of 25 carvedilol matrix tablet batches prepared via roller compaction, revealing that granule-level particle size distribution (d_{50} and d_{90}) and roll speed exerted a stronger impact on drug release than hypromellose content or tablet hardness. Unexpectedly, higher d90 values increased release, while higher d50 values decreased it, reflecting complex densification-fragmentation interactions during compression. Granules with smaller d90 (fewer large particles) allowed tighter packing and reduced porosity, thus slowing release, while granules with high d50 were softer and fragmented easily, also resulting in lower porosity and slower release. These effects were confirmed through friability analysis, compactibility testing, and compressibility plots, highlighting that tablet porosity—not just matrix composition—drives early release behaviour in hypromellose-based systems [26]. From this, we draw the argument that intermediate dissolution performance is dictated not only by excipient ratios, but also by microstructural properties modulated by RC settings, and underscores the need for PSD monitoring. Moreover, Anuschek et al. (2023) used terahertz time-domain spectroscopy (THz-TDS) as a process analytical tool to non-destructively measure granule internal structure. Their findings confirmed that granule densification signatures obtained via THz-TDS could be used to predict disintegration performance in real-time monitoring of compaction effects across granulation platforms [27]. In parallel, Matji et al. (2019) showed that manipulating the fines content in RC ibuprofen formulations had a dual impact: while some fines improved compactibility and mechanical strength, excess fines ($> 20\%$) reduced flowability and disrupted dissolution, indicating the need for tightly controlled fines levels during post-compaction sieving [23]. While in erlotinib formulations, Hwang et al. (2019) showed that fines recycling during RC improved flow and maintained tensile strength, yet excessive compaction reduced early dissolution, underlining the balance between densification and performance [28]. Several modeling studies and alternative granulation routes also support the relevance of intermediate granule-level evaluation. Comparative studies focused on the process parameters and the intermediate granules. Matsunami et al. (2023) developed surrogate models to forecast dissolution behaviour from granule-level input parameters such as bulk density, porosity, and water uptake, revealing that dry-granulated formulations, particularly those of BCS Class II drugs, exhibited slower and more variable dissolution compared to their wet-granulated analogs. These differences were attributed to more extensive granule densification and poorer wetting properties in RC systems [29]. Kim et al. (2022) used a QbD framework to map how roller force and screen size propagated through the process chain to affect dissolution variability, validating Monte Carlo-based risk modeling for roller compaction [30]. Mitchell et al. (2003) explored dry granulation using polymeric carriers like HPMC and found that matrix hydration and swelling kinetics could override densification effects and enhance dissolution of poorly soluble APIs [31]. These studies converge in realizing that granule-level structural and compositional properties shaped by RC parameters and formulation design govern disintegration and dissolution outcomes. Despite extensive research into granule attributes and their impact on tablet performance, the role of intermediate granule dissolution remains underutilized. These insights support the inclusion of granule-level dissolution testing for anticipating formulation behaviour prior to tableting. Current methodologies primarily assess tablet disintegration or dissolution rates, overlooking the diagnostic potential of granule dissolution profiles [32]. Quality by Design (QbD) underscores the significance of process understanding and CQA monitoring, with increasing interest in its application for formulation development. This framework naturally extends to encompass granule attributes and, by extension, granule dissolution analysis, though this is not always the case. As critical intermediates in these pharmaceutical production processes, granules offer an opportunity to screen formulations early in the development cycle. Establishing correlations between granule dissolution behaviour and final product performance could streamline formulation development, reduce experiment-intensive tablet testing, and provide earlier insights into formulation suitability [3, 33–39]. The USP4 flow-through cell method adequately provides a dynamic and reproducible platform for studying dissolution behaviour, particularly beneficial for poorly soluble compounds. It simulates physiological conditions with controlled fluid flow, offering distinct advantages over traditional methods like the USP2 paddle method by producing more detailed data and better replicating *in vivo* conditions. This method has shown promise in predicting the dissolution behaviour of final dosage forms based on their precursors, saving time and reducing experimental effort during formulation development. By allowing early-stage evaluation of formulations, USP4 helps optimize processing parameters and excipient combinations while ensuring reliable performance in the final dosage form [7, 33, 40–44].

With this in mind, the aim is to highlight the utility of the USP4 flow-through cell method for evaluating the dissolution behaviour of roller-compacted granules from two real pharmaceutical formulations during development. This approach will be assessed against conventional USP2 paddle dissolution testing of tablets prepared from the same granules. Using USP4 to study granule dissolution specifically addresses the industry's demand for early-stage testing aligned with the expanding QbD principles. The ability to evaluate process variables early enables the identification of potential formulation issues, optimizing workflows and supporting more informed decision-making in formulation development.

Materials and Methods

In this work, we utilized two real pharmaceutical formulations (designed for pharmaceutical products). One of the formulations contained a well soluble (BCS3 type) API Dapagliflozin and the other contained a poorly soluble (BCS2 type) API Simvastatin. Both active ingredients were provided by the industrial partner Zentiva k.s. (the composition of these mixtures is further specified only qualitatively, per request of the industrial partner). Compressibility of mixtures was studied using uniaxial tablet compression on an instrumented tablet press. Various equipment was used for dry granulation. Reynolds model was employed to obtain peak pressure and to calculate density in roller compaction experiments. To study dissolution behaviour, the flow-through dissolution cell (USP4) and paddle dissolution (USP2) were used. Disintegration kinetics were determined using static light scattering.

Pharmaceutical Mixtures

Both pharmaceutical mixtures comprise an intragranular part and an extragranular part. The intragranular blend is processed in a dry granulation stage into granules. Afterwards, the granules are admixed with the extragranular components to form a material premix ready for compression (MRC) before the tableting stage. Both mixtures were similarly prepared by the following procedure. The active ingredient was pre-conditioned with microcrystalline cellulose by manually shaking and kneading the blend in a plastic bag. The rest of the intragranular components except the lubricant were weighed into a container, and this mixture was blended using a 3D mixer Turbula T2F (Willy A Bachofen AG, Switzerland) for 5 min at 45 RPM setting. The premix containing the active ingredient was then triturated through a 1 mm sieve to the rest of the ingredients. The container was then further mixed using the Turbula for another 10 min. Lubricants were incorporated into the mixture and homogenized for an additional 3 min using the Turbula mixer. After dry granulation, the extragranular components were added and mixed with the granules for 5 min using the Turbula shortly before compression into tablets. The pharmaceutical composition of the Dapagliflozin mixture is specified for all components qualitatively in Table I. The particle size of Dapagliflozin used for majority of experiments was a d90 of 154 µm (regular particles). Two granule samples were also prepared with micronized Dapagliflozin particles, with d_{90} of 24 µm. Particle size distribution was determined using Malvern Mastersizer 2000 (Malvern Instruments, UK) equipped with a Hydro SM dispersion unit.

Table I Dapagliflozin Formulation Components (D-mixture)

Dapagliflozin mixture composition	Function
Intragranular Components	
Dapagliflozin propanediol hydrate 12.3 mg (4.9%) (equivalent to Dapagliflozin 10 mg (4.0%)	API (BCS3)
Avicel PH101 Microcrystalline cellulose	Filler
Lactose anhydrous	Filler
Crospovidone	Dry Binder
Aerosil 200	Glidant
Magnesium stearate	Lubricant
Extragranular components	
Crospovidone	Tablet binder
Aerosil 200	Glidant
Magnesium stearate	Lubricant
Tablet Weight	250 mg

The pharmaceutical composition of the Simvastatin mixture containing the poorly-soluble API is specified for all components qualitatively in Table II. The particle size of Simvastatin used in all samples that were used for experiments had a d_{90} of 28 µm.

Powder Rheometry

Powder flow tests were carried out on an FT4 Powder Rheometer (Freeman Technology, UK). Using a 23.5 mm stainless-steel conditioning blade that was fitted for every initial conditioning cycle, and all samples were weighed using in-instrument analytical balance. The following three tests were performed: Shear properties (to obtain flow function and effective angle of friction) were done with a shear cell test. Approximately 6 g of powder was introduced into a 25 mm × 10 ml split vessel. After two blade-conditioning passes, the vented piston imposed the chosen 15 kPa pre-consolidation stress, the vessel was split to the 10 ml mark and the piston replaced by the shear-cell head. The head reconsolidated the bed and then followed the standard FT4 sequence of pre-shear and five descending normal-stress steps to generate a yield locus. Wall friction test was also done with approximately 6 g of powder and conditioned in the same 25 mm × 10 ml split vessel. Following pre-consolidation with the vented piston, the vessel was left open and the piston exchanged for the wall-friction head fitted with a 316 stainless steel disc of 1.2 µm arithmetic roughness. Steady-state shear stress was recorded at a series of reducing normal stresses to construct the locus. Basic Flowability Energy test was done to obtain conditioned bulk density and flow rate index. For this test, 15 g of powder was conditioned in a 25 mm × 25 ml split vessel, then the vessel was split to 25 ml. Without changing the blade, the standard program drove the blade downward through the bed at 100 mm s^{-1} in an anticlockwise direction to capture the work required to pass through the powder bed.

Table II Simvastatin Formulation Components (S-mixture)

Simvastatin mixture composition	Function
Intragranular Components	
Simvastatin 20 mg (10.0%)	Active ingredient
Lactose Anhydrous	Filler
Avicel PH101 Microcrystalline cellulose	Filler
Pregelatinized maize starch	Dry binder
Talc	Glidant
Magnesium stearate	Lubricant
Butylhydroxyanisolum micro	Anti-microbial
Extragranular components	
Avicel PH 101	Filler
Talc	Glidant
Magnesium stearate	Lubricant
Tablet Weight	200 mg

Compressibility of Pharmaceutical Mixtures

Compressibility was determined using an instrumented Gamlen Tablet Press GTP-1 (Gamlen Tableting, United Kingdom) equipped with a 5 mm round, flat-faced die. Prior to analysis, the powder was sieved through a 2 mm mesh to disaggregate clumps. For each measurement, a 105 mg sample was weighed and manually loaded into the die. The upper punch was set to operate at a constant speed of 60 mm/min with zero hold time at the target load. Six replicate compacts were prepared for each load condition and tableting was performed in a force controlled regime to provide more uniform densification of compacts [45–47]. A series of seven compressive loads (25 kg, 50 kg, 100 kg, 200 kg, 300 kg, 400 kg, and 500 kg) were applied to the powder. These loads correspond to peak pressures from 12.5 to 250 MPa. The peak pressure (P_{max}) is calculated from the applied load (L), the acceleration due to gravity (g), and the punch radius (r) using the equation:

$$P_{max}[MPa] = \frac{(L \cdot g)}{(\pi r^2) \cdot 10^{-6}} \tag{1}$$

After ejection, compacts were allowed to relax before their dimensions and weight were measured with MT50 Multitest (Sotax, Switzerland) and analytical balance to determine the out-of-die apparent density (ρ). Densification profiles were charted using compact apparent density against the peak pressure used to form them. The out-of-die compressibility factor, K, was determined from the slope between the relationship of natural logarithm of the compact apparent density against the natural logarithm of the peak pressure. This relationship is based on the power-law equation of the Reynolds model, which can be expressed in its linear form (Eq. 2) where C is material-dependent and encompasses initial density state (ρ_0) at feeding pressure P_o [48–50].

$$\ln(\rho) = \left(\frac{1}{K}\right) \cdot \ln(P_{max}) + C \tag{2}$$

Dry Granulation Methods

The methods utilized for dry granulation in this work are roller compaction and slugging via uniaxial compression. To obtain granules, both methods were followed by crushing the prepared ribbons/slugs through a 1 mm sieve. Compressibility of mixtures was determined using uniaxial test data on instrumented tablet press.

Due to the case study nature of this work, the dry granulation method flow for sample preparation was not unified for both mixtures. This approach arose from the need to develop two pharmaceutical products, each undergoing its own early phase of formulation development. Each case addressed various experimental design aspects beyond those highlighted in this study (e.g., composition optimization, compressibility, and scale-up), with the underlying aim to complete the pharmaceutical formulation.

Slugging

Slugging in both cases was done with a hydraulic press Specac (Portman instruments, Switzerland) with a round flat-faced 10 mm diameter die. Average slug weight was 300 mg and slugs were pushed through 1 mm sieve manually to acquire granules. Peak pressure (P_{max}) for slugging process was calculated from load and die geometry used in Specac press as shown in Eq. 1. Densification of slugs was calculated using Eq. 2 where P_{max} was substituted with the value obtained from Eq. 1 for the Specac press.

Roller Compaction

For roller compaction, each mixture was processed on a differently scaled roller compactor to prepare roller compacted ribbons that would then be milled through a 1 mm sieve in the roller compactor. The roller compactors differ in settings of the compaction force parameter: The D-mixture was processed on the Mini-Pactor and this machine operates with specific compaction force (SCF) as a process parameter. The S-mixture was processed on the RCC 100×20 and this machine operates using hydraulic pressure (HP) as a process parameter. To convert between SCF and HP where applicable, in-house calibrated linear regression relationship ($\mathrm{SCF} = a \cdot \mathrm{HP} + b$) was used, which was based on both roller compactor manufacturers' data. Further specifications regarding instruments are listed in Table III.

For all samples, the collection of processed material began only after reaching steady state once feeding of material remained constant, which occurred under 5 min from start of the process. The variability of process parameters was monitored on the control panel and the fluctuation of process parameters was negligible relative to the set points.

Ribbon Envelope Density Measurement

Solid displacement method was used to measure envelope density of ribbons [51]. Using a tap density analyzer (JV1000, Pharmatron AG, Switzerland), the measurements were conducted in a 25 ml glass volumetric cylinder with a 1.82 cm inner diameter, fitted with a custom 3D printed plunger. Glass microspheres (Glass Sphere s.r.o., Czech Republic) served as the displacement medium. The tapped density of the glass microspheres was calibrated prior to sample measurement, with an error margin of less than 2%. To measure a sample, approximately 1.0 g of ribbons were placed in the cylinder with the calibrated microspheres and subjected to 750 taps. A digital caliper was used to measure the final height of the consolidated material to calculate the displaced volume.

Peak Pressure and Densification in Roller Compaction

Reynolds model principles [48–50] were used to convert applied SCF, process parameters and roller specific dimensions to P_{max} in the interface of gProms Formulated Products software (Siemens AG, Germany) using Eq. 3, where D is the roll diameter, S is gap between the rolls, K is compressibility of the powder, θ is any given angle and the integral is calculated for dimensionless force from zero angle (β) to nip angle (α). Required flow characteristics were measured with powder rheometer and compressibility determined by method in Section "Compressibility of Pharmaceutical Mixtures"was used in this calculating peak pressure. The densification of granules prepared by roller compaction was calculated using Eq. 2., but for P_{max} the value was substituted with the value obtained from Eq. 3 (specific to the roller compactor).

$$P_{max,RC} = \frac{2\,\mathrm{SCF}}{D\int_{\beta}^{\alpha_{nip}} \left[\frac{S/D}{(1+S/D-\cos\theta)\cos\theta}\right]^{K} \cos\theta \, d\theta} \quad (3)$$

Dapagliflozin Mixture Granulation and Tableting

The first sample set with Dapagliflozin mixture (D-mixture) was processed at laboratory scale with 30 g of intragranular mixture using slugging to prepare granules (Table IV).

Table III Specifications of the Roller Compactors that were Utilized for Ribbon Production from Prepared Mixtures

Apparatus	Mixture processed	Roll diameter (mm)	Roll width (mm)	Roll texture	Max Throughput (kg/h)	Compaction force parameter
Mini-Pactor®	Dapagliflozin formulation	25	2.5	Gridded	100	SCF (kN/cm)
RCC 100×20	Simvastatin formulation	10	2	Gridded	5	HP (bar)

The process was then scaled-up to roller compaction on the Mini-Pactor® (Gerteis Maschinen, Switzerland) using 4 kg of the intragranular mixture to provide the granule samples. The exact process parameters are listed in Table V. The granule sample naming was chosen as the first letter of the API used and the first letter of the granulation method that was used for preparation.

All granules were subsequently compressed into tablets. These granules were compressed using 12 × 6 mm oblong punches on a Killian T100 tableting machine (Romaco, Germany). These granules were compressed into 250 mg tablets to achieve varying compression level with low and high force parameters specified in Table VI to provide tablets with differences in densification. Tablet samples are distinguished from their granules batch by the abbreviation “LFT” (low force tablet) and “HFT” (high-force tablet). Fluctuations in tableting process parameters were not observed, and tablets were collected in steady state. Tablet hardness was measured with MT50 Multitest.

Simvastatin Mixture Granulation and Tableting

The Simvastatin mixture (S-mixture) was processed using the laboratory scale roller compactor RCC 100 × 20 (POWTEC Maschinen und Engineering GmbH, Germany). Preparation of granule samples by RC was done with 1 kg of the intragranular mixture. A scale-down of this process was performed by slugging with 30 g of intragranular mixture to provide various granules to be used in tablet compaction. Exact process parameters for each prepared granules are listed in Tables VII and VIII. The granule sample naming was chosen as the first letter of the API used and the first letter of the granulation method that was used for preparation. The process parameters to prepare first samples of Simvastatin granules on the RCC 100 × 20 by applying variable pressure are detailed in Table VII.

To acquire tablet samples, another batch of Simvastatin granules were prepared in scale-down using slugging. Granules prepared this way were then immediately pressed into

Table IV Slugging Parameters for Preparation of Granules from Dapagliflozin Mixture

Sample type	Method	Load (kg)	Slugging Peak Pressure (MPa)	Geometry	Die Diameter (mm)
DS1	Slugging using hydraulic press and sieve crushing	400	50	Round die with flat faced punch	10
DS2		2000	250		

Table V Roller Compaction Parameters for Preparation of Granules from Dapagliflozin Mixture

Sample type	Method	SCF (kN/cm)	RC Peak Pressure (MPa)	Gap Size (mm)	Roll speed (RPM)	Throughput (kg/h)
DR1	Roller compaction on Mini-Pactor®	3	52	1.5	3	6
DR2		5	87	1.5	3	6
DR3		7	122	1.5	3	6
DR1m (*)		3	53	1.5	3	6
DR3m (*)		7	124	1.5	3	6

*DR1m and DR3m granule samples contained micronized Dapagliflozin API

Table VI Tablet Preparation Parameters for Dapagliflozin Mixture Granules

Sample type	Granules origin	RC Peak Pressure (MPa)	Tablet Punches	Tableting Precompression Force (kN)	Tableting Main compression Force (kN)
DR1-LFT	Roller compaction on Mini-Pactor®	52	12 × 6 mm oblong punch	1.8	7.5
DR1-HFT		52		1.8	11.5
DR2-LFT		87		1.8	7.5
DR2-HFT		87		1.8	11.5
DR3-LFT		122		1.8	7.5
DR3-HFT		122		1.8	11.5
DR1m-LFT		53		1.8	7.5
DR3m-LFT		124		1.8	7.5

Table VII Roller Compaction Parameters for Preparation of Granules from Simvastatin Mixture

Sample type	Method	HP (bar)	RC Peak Pressure (MPa)	Gap size (mm)	Roll speed (RPM)	Throughput (kg/h)
SR1	Roller compaction on RCC 100×20	50	96	2	5	1.5
SR2		250	480	2	5	1.5

Table VIII Slugging and Tablet Preparation Parameters for Simvastatin Mixture

Sample type	Granules origin	Slugging Load (kg)	Slugging Peak Pressure (MPa)	Tableting method	Tableting Load (kg)	Tableting Pressure (MPa)
SS1T	Slugging using hydraulic press and sieve crushing	400	50	Hydraulic press	1400	175
SS2T		800	100			
SS3T		1200	150			
SS4T		1600	200			
SS5T		2000	250			

200 mg tablets right away at only one compression force using the Specac hydraulic press in a 10 mm die with flat faced punches and the details are specified in Table VIII. The tablet samples are abbreviated with "T" relative to their respective granules batch. Fluctuations in load application were not observed because slugging was done in force-controlled regime. Tablet hardness was measured with MT50 Multitest (Sotax, Switzerland).

Dissolution Methods

Methods for dissolution of granules and tablets were developed. The dissolution properties of select granules were investigated using the flow-through dissolution cell USP4 CE7 (Sotax, Switzerland). For the USP4 method, a powder cell assembly as recommended by Sotax was used for the granules testing. The active ingredients in the formulations required different test conditions and dissolution media, and because of that, each method is described further in the following subsections. For tablets, the dissolution properties were examined using the USP2 paddle dissolution test with the AT7 (Sotax, Switzerland). Samples were collected at different intervals, and methods for content analysis were developed on HPLC equipment. Blank samples were acquired from blank cells in the dissolution. Similarity to reference powder was statistically examined by the f2 similarity factor defined as:

$$f_2 = 50 \cdot \log_{10}\left(\frac{100}{\sqrt{(1 + (1/n) \cdot \sum_{t=1}^{n} \left(R_t - T_t\right)^2}}\right) \tag{4}$$

Dapagliflozin Granules Dissolution Experiments

The ribbons containing the Dapagliflozin formulation were processed through a 1 mm sieve to produce granule samples for testing. Each powder cell was loaded with 100 mg of granule sample. The dissolution medium was plain distilled, deaerated water tempered at 37 °C. Since Dapagliflozin is a well-soluble drug, the dissolution tests were carried out with 8 ml/min flow rate. Samples were collected 7 times in intervals of [2.5; 2.5; 2.5; 7.5; 10; 15; 20 min] over the course of 60 min. Dissolution was done in open-loop mode, and samples were collected in triplicates.

Dapagliflozin Tablet Dissolution Method

The dissolution tests for Dapagliflozin tablets were done accordingly. The dissolution test was performed in a medium containing 500 mL of phosphate buffer of pH 6.8 (prepared from 6.81 g/l KH_2PO_4 and 0.9 g/l NaOH) at 75 RPM (lower paddle speed of 50 RPM exhibited coning of the powder). Sample collection occurred at [2; 3; 5; 5; 5; 5; 5; 15] minute intervals over the course of 45 min, followed by an increase in paddle stirring to 150 RPM and extra sample collection at [5; 10] minute intervals for a total of 60 min. The replaced volume was equal to sampling volume, which was 5 ml. The blank was taken from prepared dissolution medium.

Dapagliflozin Content Analysis

The chromatographic analyses of all experiments were done by High Performance Liquid Chromatography (HPLC) with the setup of ACQUITY UPLC M-class system (Massachusetts, USA). The used column was a C18 column (Gemini 3u C18 110 A 150 × 4.6 mm, Phenomenex, USA). The elution was isocratic with a mobile phase of 60:40 (V/V) of Acetonitrile: Phosphate buffer (0.25% (w/V) KH_2PO_4 adjusted to 3.5 pH with Phosphoric acid). A flow rate of 1 ml/min was chosen and the absorption was measured at 227 nm wavelength. To quantify Dapagliflozin, a calibration curve was plotted by preparing a dilution series with a measuring range from 0 to 0.1 mg/ml. For this, Dapagliflozin was dissolved in 40:60 (V/V) ACN:H_2O.

Simvastatin Granules Dissolution Method

The ribbons containing Simvastatin formulation were processed through a 1 mm sieve to produce granules for testing. When using a general approach with the testing conditions of a 30 mg sample at 16 mL/min flow rate in pH 6.8 phosphate buffer (0.68% (w/V) KH_2PO_4 and 0.09% (w/V) NaOH) insufficient resolution of the dissolution data was observed. Therefore, a method was developed to obtain better dissolution resolution. Per the suggestion made by Singla et al. [52] and in-house verification the most effective dissolution medium was chosen to be pH 6.9 phosphate buffer (0.09% (w/V) NaOH and 0.8% (w/V) $Na_2HPO_4*2H_2O$) with a wetting agent of 0.1% (w/V) Sodium dodecyl sulfate (SDS). With this method, samples were collected 9 times in [2; 2; 2; 4; 4; 4; 6; 9; 10] minute intervals over the course of 45 min.

Simvastatin Tablet Dissolution Method

The dissolution tests for simvastatin tablets were studied in two different dissolution media. One was done as a standard dissolution test containing 900 mL of phosphate buffer of pH 6.8 (prepared from 6.81 g/l KH_2PO_4 and 0.9 g/l NaOH) at 75 RPM with sample collection at [5; 15; 15; 15; 15; 15; 15] minute intervals over the course of 90 min. Since this also provided insufficient evidentiary power, the second experiment setup utilized 900 mL of the same phosphate buffer that also contained 0.1% of sodium dodecyl sulfate as a solubilizer. The second experiment was done at 75 RPM with sample collection at [1; 1; 2; 2; 4; 5; 5] minute intervals over the course of 20 min. The replaced volume was equal to sampling volume, which was 5 ml. The blank was taken from prepared dissolution medium.

Simvastatin Content Analysis

The chromatographic analyses of all experiments were done by High Performance Liquid Chromatography (HPLC) with the setup of Shimadzu LC-20 HPLC system (Shimadzu, Japan). The column used was a C18 column (Kinetex 5u C18 100 A 150 × 4.6 mm, Phenomenex, United States of America). The elution was isocratic with a mobile phase of 30:70 (V/V) of double distilled water(ddH_2O):ACN. A flow rate of 1 mL/min was chosen, and the absorption was measured at 238 nm wavelength. To quantify Simvastatin, a calibration curve was plotted by preparing a dilution series with a measuring range from 0 to 0.150 mg/mL. For this, Simvastatin was dissolved in 30:70 (V/V) ddH_2O:ACN.

Methodology of Studying Disintegration Kinetics

The disintegration mechanics of tablets were studied by in-situ real-time monitoring using static light scattering (SLS) of sampled materials by utilizing a Mie-theory scattering model. The SLS was done using a Mastersizer 3000 laser diffractometer machine with the Hydro MV dispersion unit (Malvern Panalytical Ltd., UK). The dispersion unit was filled with 500 mL of distilled water at lab temperature, and the stirrer was set to 2000 RPM (to prevent particle sedimentation). Because microcrystalline cellulose was the major excipient in both formulations and is insoluble in water, it was chosen as the calibration material for laser obscuration. The particle type was classified as non-spherical, with a refractive index of 1.468 and an absorption index of 0.010. The dispersant medium (water) refractive index was set to 1.330. Sample duration measurement was set to 10 s, and the delay between measurements to 9 s. Calibration curves for laser obscuration for both mixtures were captured by the addition of 50 mg samples up to 250 mg. The obtained laser obscuration and particle size distribution values were employed to compare the tablet disintegration kinetics. The results are presented either in a chart of cumulative weight fraction of each size class over time or as a weight distribution at specific time point. The specific size classes are specified in each example [53].

Results and Discussion

Granules and tablets prepared from the pharmaceutical mixtures were examined for their densification, dissolution and disintegration behaviour. Densification was studied with instrumented tablet press to find compressibility of the formulations. Dissolution was done using the flow-through dissolution cell (USP4) and paddle dissolution (USP2) and disintegration studies were done with SLS method.

Compressibility of Dapagliflozin Formulation

The densification measurement was done with the instrumented tablet press method for D-mixture containing regular and micronized particles of Dapagliflozin. The relationship between peak pressure and the resulting out-of-die envelope density for both samples are presented in Fig. 1. Out-of-die

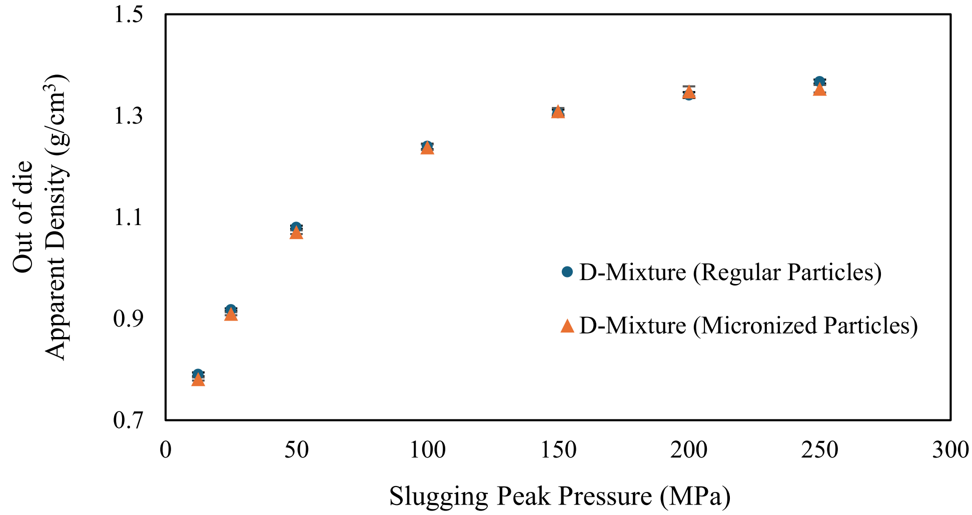

Fig. 1 Densification profile of D-mixture with regular particles (circle, d90 = 154 µm) and micronized particles (triangle, d90 = 24 µm). Dapagliflozin PSD does not affect densification of the formulation

Table IX Log–log Pressure-density Regression Details to Determine Compressibility K of D-mixture

Sample	Slope k	p-value (zero slope)	Material Constant C	R^2	Compressibility K (1/k)
D-mixture (Micronized Particles)	0.187	1.2×10^{-5}	−0.683	0.983	**5.35**
D-mixture (Regular Particles)	0.190	1.8×10^{-5}	−0.703	0.981	**5.25**

apparent density increased steadily with peak pressure, rising from 0.79 g/cm^3 at 12.5 MPa to 1.37 g/cm^3 at 250 MPa. To quantitatively compare the two profiles, a paired t-test was performed on the density values. The paired t-test across the seven pressures indicated no significant overall density difference ($\Delta = 0.0045$ g/cm^3; $t = 1.54$, $df = 6$, $p = 0.17$). Therefore, the initial API particle size did not significantly influence the overall compressibility of the powder mixture. Afterwards, to obtain compressibility values K, this data was log–log transformed and fitted by linear regression according to Eq. 2 and the result is presented in Table IX. Both size classes of the API used in the mixtures have very similar compressibility constants, indicating that particle size of the API does not affect the densification of the formulation within the studied pressure range.

Table X compares the envelope densities predicted from the Reynolds model Eq. 2 with direct measurements for five samples. Deviations range from –0.03 to + 0.08 g/cm^3, with an average bias of + 0.037 g/cm^3. A paired t-test shows the difference is not statistically significant ($p = 0.12$), and the calculated and measured values correlate strongly ($R^2 = 0.93$). These results show that the model calculations provide a good estimate of envelope density within experimental uncertainty for the compared samples.

Dissolution Behaviour of Dapagliflozin Formulation Granules and Tablets

All Dapagliflozin formulation granules were examined for their dissolution behaviour using the USP4 flow-through method, and the dissolution profiles are shown on Fig. 2. The rather anticipated difference is seen in the faster dissolution

Table X Comparison of D-mixture Samples Calculated and Measured Envelope Density at Respective Peak Pressure

Sample	RC Peak Pressure (MPa)	Slugging Peak Pressure (MPa)	Calculated Envelope Density (g/cm^3)	Measured Envelope Density (g/cm^3)
DS1	-	50	1.040	1.070 ± 0.003
DS2	-	250	1.417	1.353 ± 0.007
DR1	52	-	1.030	0.954 ± 0.030
DR2	87	-	1.135	1.110 ± 0.045
DR3	122	-	1.211	1.160 ± 0.054
DR1m (*)	53	-	1.018	-
DR3m (*)	124	-	1.192	-

Fig. 2 USP4 flow-through dissolution profiles of Dapagliflozin granulates samples with regular API – DS1 (Square); DS2 (Triangle); DR1 (Asterisk); DR2 (Rhombus); DR3 (Cross) and of Dapagliflozin granulates with micronized API – DR1m (Circle); DR3m (Plus)

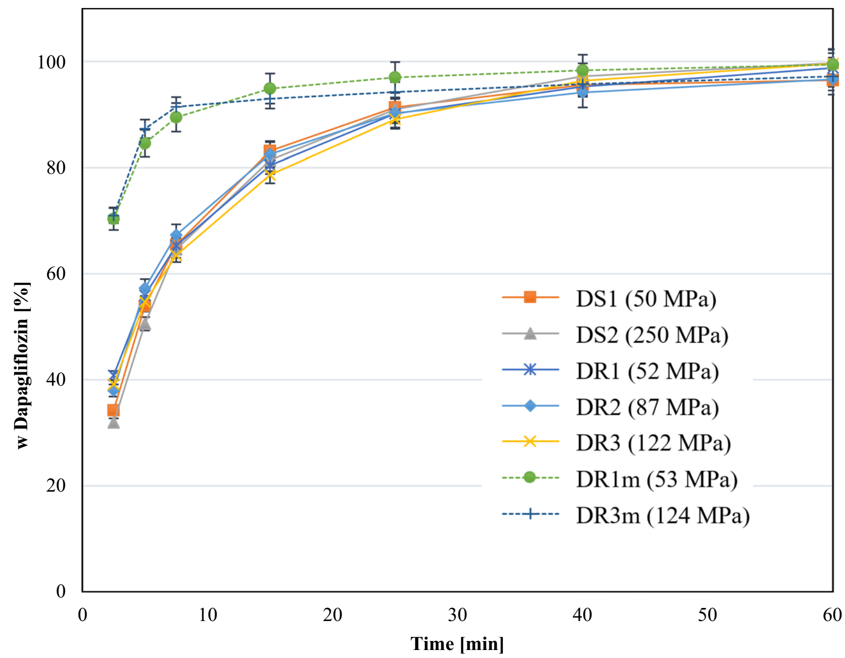

rate of samples DR1m and DR3m when compared to the other samples. This effect is due to the micronization of API particles. These results also collectively indicate that the granule samples prepared by the slugging method are equally suitable for generating dry granulation samples intended for screening experiments. While roller compaction is often preferred for scale-up, Mitchell et al. (2003) and Dehont et al. (1989) also successfully employed slugging, supporting our observation that for simple screening of highly soluble drugs like Dapagliflozin, slugging can provide comparable intermediate materials [31, 54]. Overall, the results of all tested granule samples, that did not contain micronized API, show a similar dissolution rate. Moreover, the level of densification between samples DS1 and DS2 (Table X) is the largest but their dissolution profile is nearly identical. This is indicative of an insignificant effect of compaction pressure on the dissolution rate of Dapagliflozin from granules.

The granules that were prepared with roller compaction were further pressed into tablets and their dissolution behaviour was studied using the USP2 paddle method. Figure 3 illustrates a consistent dissolution rate across all tablet samples, irrespective of granule density inside the samples (Table X), tableting pressure and tablet hardness of the samples (Table XI).

The key difference introduced by tableting is the anticipated nominal slowdown of the dissolution rate across all samples. The dissolution of the tablets is equally balanced after around the 10-min mark, once the macro-disintegration of all tablet samples was finished and the dissolution profiles have achieved consistent release. In fact, this behaviour can also be supported by the tablet disintegration analysis in Fig. 4. When comparing the disintegration of the tablets with the most divergent compaction and tableting pressures, DR1-LFT and DR3-HFT, it is evident that the disintegration rates are rapid and with similar kinetics. Because of this, the disintegration profiles of these tablets over the course of 8 min imply that similar starting conditions are present for the dissolution of the formulations, regardless of the pressure used in compaction or tableting. Tablets containing micronized API are again seen with a faster dissolution rate, as anticipated. The tablet dissolution profiles are therefore also indicative of a minimal effect of compaction pressure on the rate of Dapagliflozin release from the samples. However, Fig. 3 also reveals incomplete release even after applying infinity spin (increase of paddle speed to 150 RPM). The released amount of Dapagliflozin in the dissolution profiles plateaus at ~ 91%. The rationale behind the infinity spin was to elucidate the effect of extragranular excipients and the incomplete release can be likely attributed to magnesium stearate [55, 56].

Overall, the primary trend observed in the API release across both testing methodologies indicates that the dissolution rate of a highly soluble API, such as Dapagliflozin, remains unaffected by the compaction pressure applied during dry granulation and the subsequent tableting pressure applied to these granules. This finding suggests that the dissolution testing outcomes did not show significant improvement from an expanded design of experiments, as the dissolution rates were largely invariant to the density and compaction levels applied. Since this could be identified earlier in development using the USP 4 flow-through dissolution method on the granules, conclusions about the

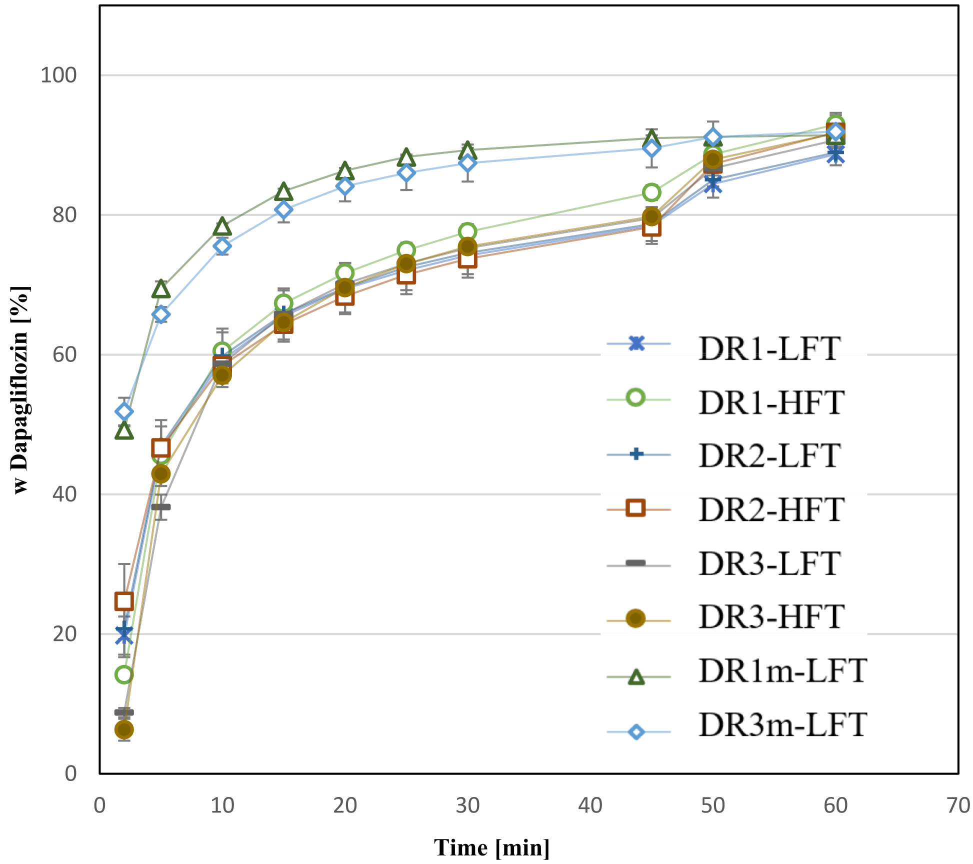

Fig. 3 USP2 paddle dissolution profiles of Dapagliflozin tablets – DR1-LFT (Asterisk); DR1-HFT (Circle); DR2-LFT (Plus); DR2-HFT (Square); DR3-LFT (Minus); DR3-HFT (Full Circle) and of Dapagliflozin tablets with micronized API—DR1m-LFT (Triangle); DR3m-LFT (Rhombus)

Table XI Tablet Hardness for Samples of the Dapagliflozin Granules

Sample	Hardness (N)
DR1-LFT	125 ± 10
DR1-HFT	155 ± 12
DR2-LFT	110 ± 9
DR2-HFT	140 ± 11
DR3-LFT	100 ± 9
DR3-HFT	130 ± 11
DR1m-LFT	120 ± 10
DR3m-LFT	95 ± 9

dissolution behaviour of the Dapagliflozin formulation can be drawn more efficiently based on these findings. Subsequent optimization efforts in the tableting phase can then be more targeted, focusing primarily on pharmaceutical engineering aspects such as the ease of tableting and the mechanical properties of the final tablets. This strategic focus is expected to improve overall development efficiency.

Compressibility of Simvastatin Formulation

The densification measurement was done with instrumented tablet press for S-mixture formulation. The relationship between peak pressure and the resulting out-of-die envelope density for prepared compacts is presented in Fig. 5. Out-of-die envelope density increased with peak pressure from 1.01 g/cm^3 at 12.5 MPa and reaching 1.41 g/cm^3 at 250 MPa. The density-pressure data were analysed individually by log–log regression (Eq. 2). The fitting yielded the corresponding compressibility constant (Table XII), K = 9.62, indicating a slower densification rate than observed for the D-mixture.

Afterwards, the peak pressure corresponding densities were calculated for prepared granule samples; however, it was not possible to compare them against ribbon density for roller compacted samples (Table XIII). This was because the ribbon was not formed uniformly during the compaction process. Because of this, ribbon envelope density for S-mixture ribbons was not determined by the solid displacement method, since the measured values would not be reproducible, as the sample variability of the non-uniform material would not meet the acceptance criteria of 5% RSD, as mentioned by Marinko et al. (2024) [51].

For the comparison of calculated and measured slug envelope densities, deviations range from –0.044 to + 0.009 g/cm^3, with an average bias of 0.004 g/cm^3. A paired t-test shows the difference is not statistically significant ($p = 0.68$), and the calculated and measured values correlate strongly ($R^2 = 0.97$). This is in agreement with

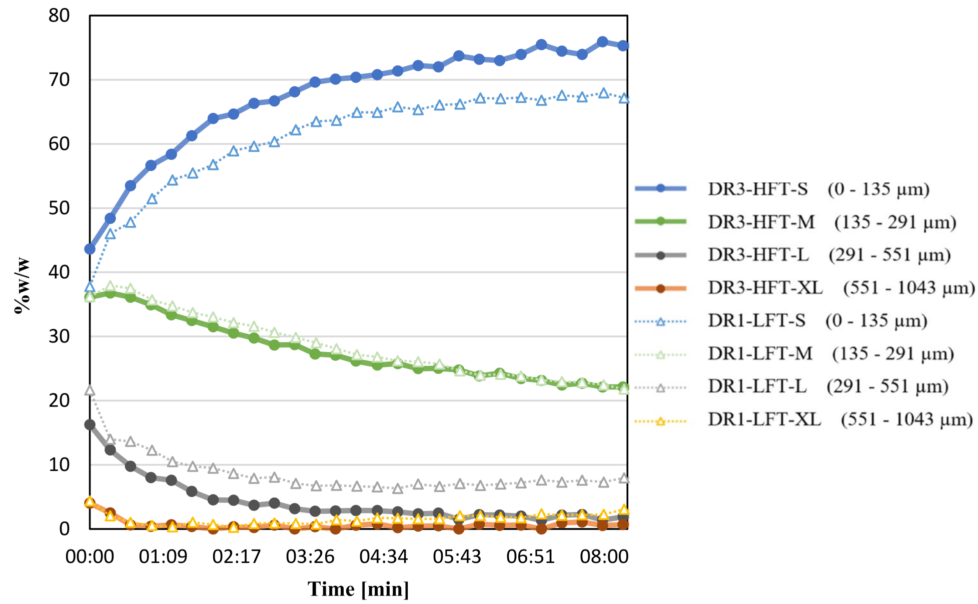

Fig. 4 Comparison of DR1-LFT (Triangles) and DR3-HFT (Circles) tablet disintegration. Each curve represents settling of particles by mass percentage of a tablet in a size class

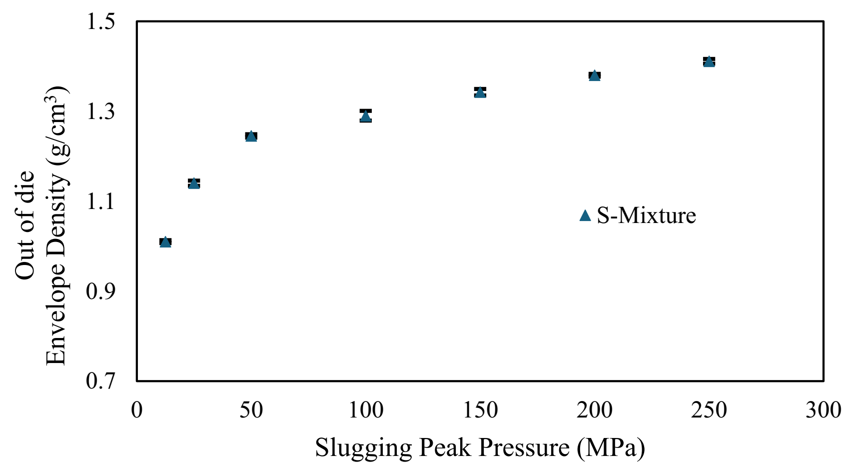

Fig. 5 Densification profile of S-mixture

Table XII Log–log Regression Details to Determine Powder Compressibility K of S-mixture

Sample	Slope k	p-value (zero slope)	Material Constant C	R^2	Compressibility K (1/k)
S-mixture	0.104	5.6×10^{-5}	−0.223	0.970	**9.62**

findings presented by Reynolds et al. (2010) [48–50] when looking at the obtained slug data. In confidence with the previous results shown for D-mixture, the predicted ribbon density at 96 and 480 MPa (SR1, SR2) with roller peak pressure estimation fits well within the compressibility

Table XIII Comparison of S-mixture Samples Calculated and Measured Envelope Density at Respective Peak Pressure

Sample	RC Peak Pressure (MPa)	Slugging Peak Pressure (MPa)	Calculated Envelope Density (g/cm^3)	Measured Envelope Density (g/cm^3)
SR1	96	-	1.285	-
SR2	480	-	1.519	-
SS1	-	50	1.201	1.245 ± 0.003
SS2	-	100	1.291	1.291 ± 0.010
SS3	-	150	1.347	1.342 ± 0.007
SS4	-	200	1.388	1.380 ± 0.003
SS5	-	250	1.420	1.411 ± 0.005

data. This supports claims that slug experiments can serve as a practical surrogate for powder compressibility [48, 57–59].

Dissolution Behaviour of Simvastatin Formulation Granules and Tablets

Conventional dissolution method for Simvastatin release was not discriminative enough. This is shown in Fig. 6, where the dissolution profiles of the least and most compacted granule samples reached < 50% API release in 90 min. Using the granules prepared at 50 bar, we developed a method with a wetting agent. The optimal flow rate for this medium was chosen as 4 mL/min (Fig. 7), as it provides discriminative resolution for sample analysis while also resulting in over 80% of API release after 15 min and full release by the 45-min mark.

The granules of the Simvastatin formulation that were prepared by roller compaction were then tested with the optimized method for their dissolution behaviour against uncompacted powder mixture using the USP4 method. The recorded dissolution profiles are shown in Fig. 8. The granules display a trend of slower release profiles at the 10 and 15 min mark. This trend is more profound depending on the level of densification in the granules when compared to the uncompacted mixture, with the largest difference displayed by SR2 formulation. Quantitative assessment with the similarity factor f_2 showed that SR1 is similar ($f_2 = 70.1$), while SR2 granules had the $f_2 = 48.8$ below 50, therefore not similar. The SR2 profile lagged behind the reference by 10–16% dissolved up to 20 min, and these early deviations affected the f_2 calculation, showing that for the poorly soluble Simvastatin (BCS2), higher compaction pressure in the SR2 granules led to this slower release profile. The higher densification likely reduces intragranular porosity and the effective surface area available for solvent penetration and drug dissolution, consistent with principles outlined by Sun et al. (2006) and Zinchuk et al. (2004) [4, 60]. Therefore, the effect of compaction pressure in this experiment is established.

Because of this, additional investigation into how granules contribute to dissolution involved separating the

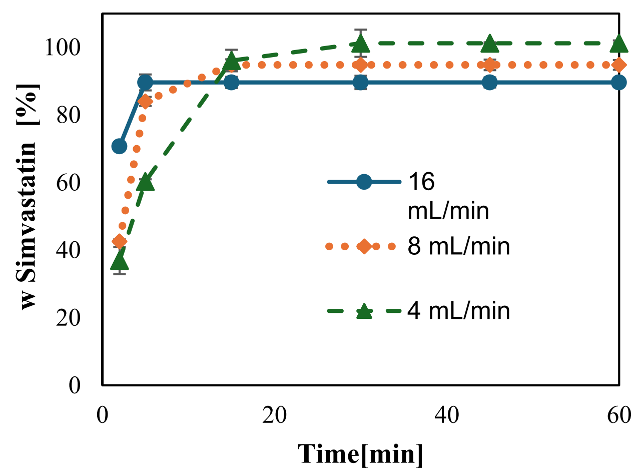

Fig. 7 Updated USP4 dissolution method with a wetting agent yields better dissolution profiles. Granulate SR1 tested with different flow rates: Circle – 16mL/min; Rhombus – 8mL/min; Triangle – 4mL/min

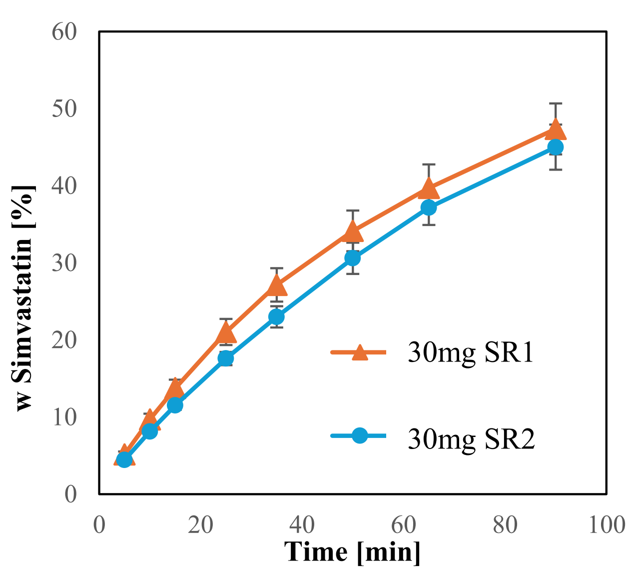

Fig. 6 Unsatisfactory resolution for Simvastatin release in USP4 using conventional method (at 16 mL/min flow rate in pH 6.8 phosphate buffer (0.68% (w/V) KH_2PO_4 and 0.09% (w/V) NaOH)). Triangle – Granulate SR1; Circle – Granulate SR2

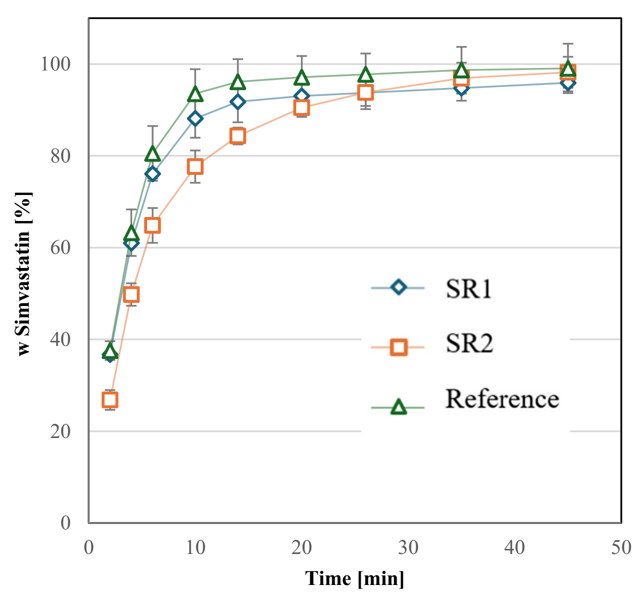

Fig. 8 Dissolution of Simvastatin of non-sieved samples with different densification in USP4 flow-through dissolution – SR1 (Rhombus); SR2 (Square); Reference mixture (Triangle)

Table XIV Sieve Analysis of SR1 and SR2 Granules Including Powder Rheometer Results

Sample type	Size Class	Weight fraction (%)	Flow Function	Bulk Density (kg/m^3)	Flow Rate Index	Angle of internal friction (°)
Reference	Unsieved	100	7.2 ± 0.4	489 ± 51	3.2	35.5 ± 1.3
SR1	Unsieved	100	13.1 ± 1.1	608 ± 42	2.3	34.3 ± 1.4
SR2	Unsieved	100	13.8 ± 1.5	611 ± 47	2.4	36.1 ± 1.6
SR1S	< 250 µm	13	9.0 ± 0.4	614 ± 53	2.9	33.4 ± 1.3
SR1M	250–560 µm	35	14.3 ± 1.2	598 ± 61	1.9	35.1 ± 1.2
SR1L	560–1000 µm	52	16.0 ± 0.7	620 ± 36	1.6	35.9 ± 1.3
SR2S	< 250 µm	12	9.2 ± 1.0	634 ± 57	2.7	34.8 ± 1.6
SR2M	250–560 µm	38	14.9 ± 1.3	598 ± 49	1.8	35.8 ± 1.7
SR2L	560–1000 µm	50	16.8 ± 1.1	593 ± 54	1.5	36.2 ± 1.4

granules by sieve analysis. The granules were separated into three size classes: 560–1000 µm, 560–250 µm and < 250 µm. The unsieved granules, each new granule size class, and the reference uncompacted powder were also examined for basic flow properties using a powder rheometer. The details of this analysis are shown in Table XIV. This analysis revealed that dry granulation of the reference mixture increased the bulk density of the powder, which is expected with increased granularity [61, 62]. To quantify this observation, bulk-density means (n = 3) were compared with Welch two-sample tests. The SR1 unsieved granules were 119 kg/m^3 denser than the uncompacted blend ($p = 0.037$; Cohen's $d = 2.55$, a 24% gain), while the SR2 unsieved material showed an increase of 122 kg/m^3 ($p = 0.039$; Cohen's $d = 2.49$, a 25% rise). The angle of internal friction remained similar in all cases, as that can be attributed to composition [63, 64]. However, each size class behaves differently in terms of flow function and flow rate index, where increasing granule size exhibits less cohesive and more free-flowing behaviour compared to the reference powder mixture [65, 66]. A Spearman rank-correlation applied to the ordered classes (Reference—S—M—L) supports this monotonic trend ($\rho = 0.95$, $p = 2.3 \times 10^{-6}$). Each separated size class is distinguished from the original sample by the abbreviations "L" for large, "M" for medium and "S" for small.

All of the sieved granule samples were also examined for dissolution behaviour. Firstly, we will generally compare the samples at their densification levels. The dissolution profiles of different classes of SR1 againsts the unsieved counterpart and the reference powder mixture are shown in Fig. 9. In the amount released over time, a very slight slowdown depending on the size class across all curves from the reference powder is observed in the nominal means at the 10 and 15 min mark. If the same comparison for the dissolution profiles of the SR2 sieved and unsieved samples, and the reference powder mixture (Fig. 10) is made, we observe the differences between each sample from the reference powder to be more pronounced.

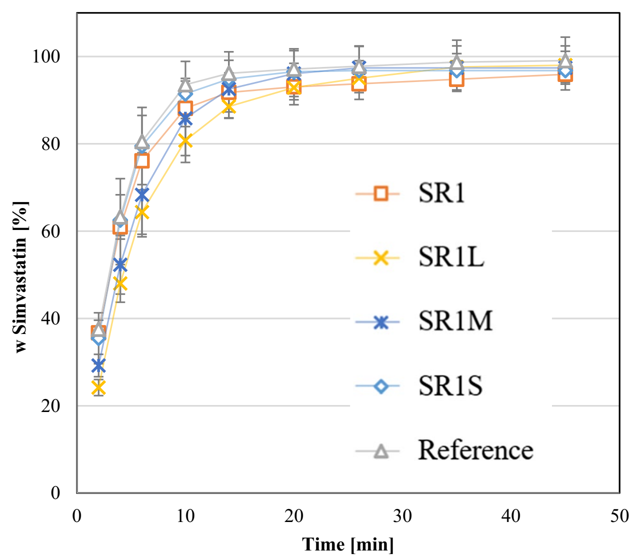

Fig. 9 USP4 flow-through dissolution profiles of Simvastatin granules prepared at 96 MPa – SR1 (Square); SR1L (Cross); SR1M (Asterisk); SR1S (Rhombus); Reference mixture (Triangle)

The general trend of slowdown is attributed to the rate of disintegration which depends on densification and granule size [67, 68]. To elucidate the significance of the slowdown from reference powder for all samples compared, dissolution curve similarity f_2 factors were calculated and presented in Table XV. For SR1 granule samples, only the largest class failed the similarity criteria (below $f2 = 50$). The similarity for each size class and unsieved sample shows the slight trend observed in the dissolution profiles. It can be concluded that the densification of these samples by roller compaction produces granules with very similar dissolution profiles to the reference powder (except the largest class). With SR2 granule samples, the dissimilarity to reference powder is more evident in the f_2 factor values and only the smallest size fraction aligned in similarity to the reference powder, which is also evident in the

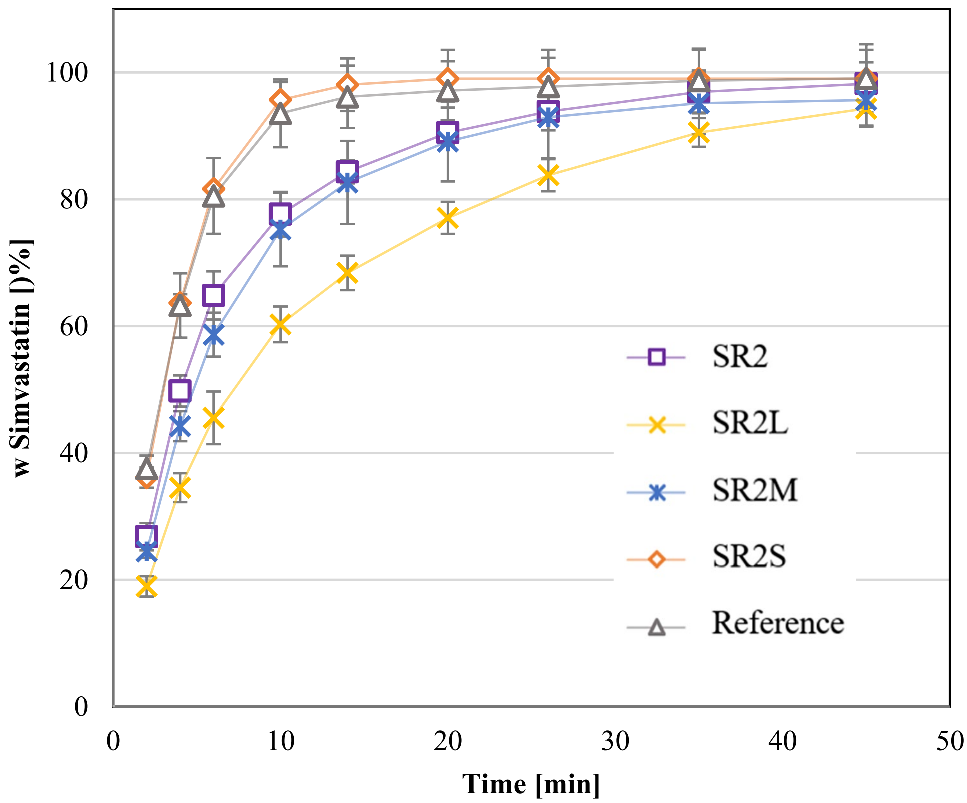

Fig. 10 USP4 flow-through dissolution profiles of Simvastatin granules prepared at 480 MPa – SR2 (Square); SR2L (Cross); SR2M (Asterisk); SR2S (Rhombus); Reference mixture (Triangle)

Table XV Similarity f2 Factors of Granules Against Reference Powder

Sample compared against Reference	Size Class	f_2 factor
SR1—bulk granules	Unsieved	70.1
SR1S	< 250 µm	86.4
SR1M	250–560 µm	58.1
SR1L	560–1000 µm	49.6
SR2—bulk granules	Unsieved	48.8
SR2S	< 250 µm	88.6
SR2M	250–560 µm	43.4
SR2L	560–1000 µm	31.5

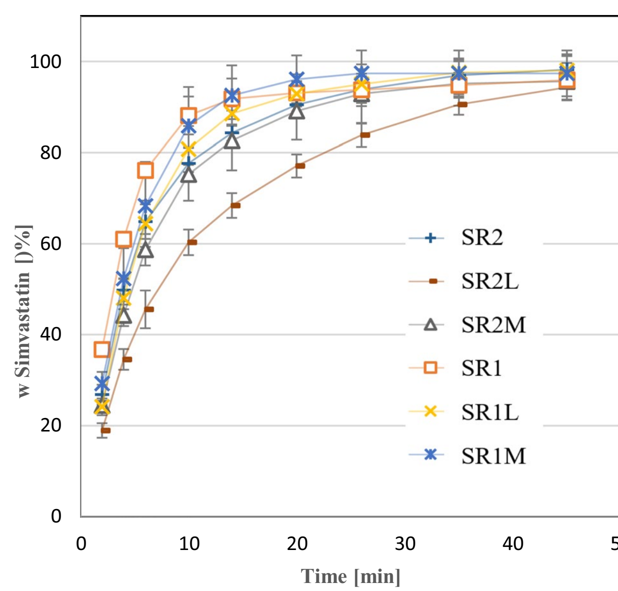

Fig. 11 Comparison of the USP4 flow-through dissolution profiles Simvastatin granules prepared at different compaction pressures – SR2 (Plus); SR2L (Minus); SR2M (Triangle); SR1 (Square); SR1L (Cross); SR1M (Asterisk)

dissolution profile. Therefore, the densification of these granules show dissolution slow-down from the reference powder.

Interestingly in both cases, the SR1S and SR2S granules that contain the smallest particles exhibit very similar dissolution profile to the reference powder mixture. This behaviour is also explainable by contamination of the granules with uncompacted powder, which also shows a similar dissolution rate. Such contamination is documented to occur between material feeding and densification into ribbons (due to underfeeding of the rolls) [69]. Contamination may also occur during the roller compaction process itself, as the densification of ribbons can be imperfect and ribbon failures such as ribbon sticking or splitting is prone to happen depending on composition of formulations as discussed by Marinko et al. (2024) [51].

Secondly, we will compare the dissolution profiles between the samples of formulations SR1 and SR2 together in more detail. Dissolution profiles are shown in Fig. 11 (excluding the reference powder and smallest size classes of the granules for clarity). The f2 similarity factors were calculated between for comparison of SR1-SR2 in each individual size classes in Table XVI. The f2 similarity factors have also been calculated between unsieved granules and their sieved samples in Table XVI. We observe a difference in the dissolution profiles of bulk SR1 and SR2 released amount of simvastatin at 10 and 15 min of which is around 10% from their means. However, the f2 factor comparison of SR1-SR2 bulk samples suggests dissolution similarity with the value 55.5 (slightly above $f_2 \geq 50$). Next, we observe that the dissolution rate of the larger granules in the SR2L sample slowed down noticeably more from the unsieved granules of SR2 and that is supported by the dissimilar f2 factor as well. Interestingly SR2S shows dissimilarity to SR2 bulk granules, supporting the claim about contamination of fines in the smallest size class. In both cases, the medium granules show a dissolution similarity compared to their unsieved counterparts.

These data draw an interesting perspective on the possible optimization of the formulation. The sieve analysis and rheometer results (Table XIV) indicated that while increasing granule size improved flow properties (higher flow function), this benefit came with a clear trade-off for the Simvastatin formulation, as larger granules (SR1L, SR2L) demonstrated slower dissolution rates (Figs. 9, 10) [1, 70, 71]. This underscores the value of intermediate granule dissolution testing, as it allows for the early identification and balancing of competing properties like flowability and drug release during process optimization This balancing act is a recognized challenge in RC, where improving flowability, often achieved with larger granules, must be weighed against potential negative impacts on other critical attributes like tabletability or dissolution, as discussed by Smrcka et al. (2015) or Mansoor and Stepanek (2006) [72, 73]. Consideration should be made that the flow properties of both samples are more advantageous with larger granule size, which is beneficial in the processing that follows after roller compaction (such as tableting). Analysis of the SR2 granules suggests utilizing a smaller mesh size in sieving to support dissolution. At the same time, both granules would benefit from repurposing the smallest size class for re-compaction to achieve granules with unified properties.

Table XVI Similarity f2 Factors Between Each Individual Size Class (SR1-SR2 column), Between Bulk and Sieved Samples of SR1 (SR1-SR1 column) and SR2 (SR2-SR2 column)

Size Label	SR1–SR2 f_2	Compared	SR1-SR1 f_2	Compared	SR2-SR2 f_2	Compared
Bulk	55.5	SR1-SR2	100	SR1-SR1	100	SR2-SR2
S	78.6	SR1S-SR2S	77.6	SR1-SR1S	47.0	SR2-SR2S
M	56.9	SR1M-SR2M	64.4	SR1-SR1M	73.4	SR2-SR2M
L	42.2	SR1L-SR2L	55.4	SR1-SR1L	44.0	SR2-SR2L

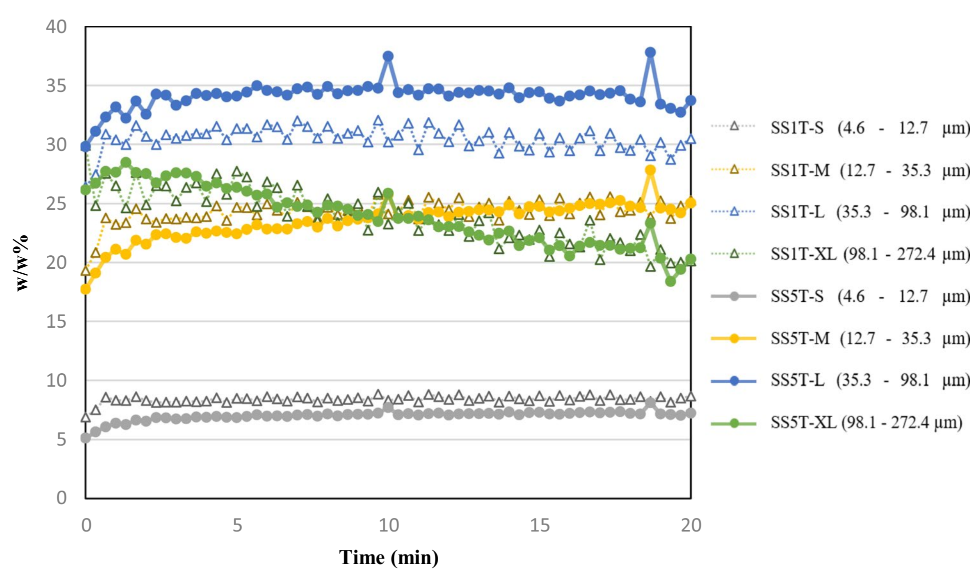

Fig. 12 Comparison of SS1T (Triangles) and SS5T (Circles) tablet disintegration. Each curve represents settling of particles by mass percentage of a tablet in a size class

The SS1T to SS5T tablet disintegration and dissolution behaviour was also studied. Figure 12 shows the disintegration kinetics of the tablets that contained granules prepared with the most divergent compaction pressures, SS1T and SS5T, we can see that the primary disintegration is very rapid (under 5 min) for both formulations. At the 10 min mark, both formulations exhibit a size class swap during secondary disintegration between the XL and M sizes. SS5T provides slightly more of the XL and L fragments vs M and S fragments in comparison to SS1T. Nevertheless, the differences are small, and from these data, we can establish that the starting conditions for the tablet dissolutions are unaffected by differences in compaction pressure.

In the tablet dissolution experiment that included a wetting agent (Fig. 11), we observe dissolution profiles for Simvastatin release with a trend depending on the peak pressure used in granulation. The tablet hardness for all tablets was similar and had a small spread, with combined mean of 114 ± 12 N. Therefore, the tablet hardness is unlikely to affect the interpretation. The most noticeable difference in the curves is observed for the dissolution of the SS1T and SS5T sample. The results of the tablet dissolution correspond to the effect shown in the granule dissolution of the Simvastatin formulation, as was expected. Interestingly, while the tablet disintegration kinetics appeared rapid and broadly similar regardless of the granule compaction pressure (Fig. 12), the subsequent dissolution profiles showed clear rank-order differences correlating with the densification (Fig. 13). This highlights that for this poorly soluble formulation, the properties imparted to the granules during roller compaction, specifically their density, carry over onto the tablets and are the dominant factors controlling the drug release rate, rather than the speed at which the tablet breaks apart initially. This reinforces the conclusions drawn by Rajkumar et al., whose work examining the stresses involved in RC and subsequent tableting showed the significant impact of the initial granulation step on final tablet performance [32].

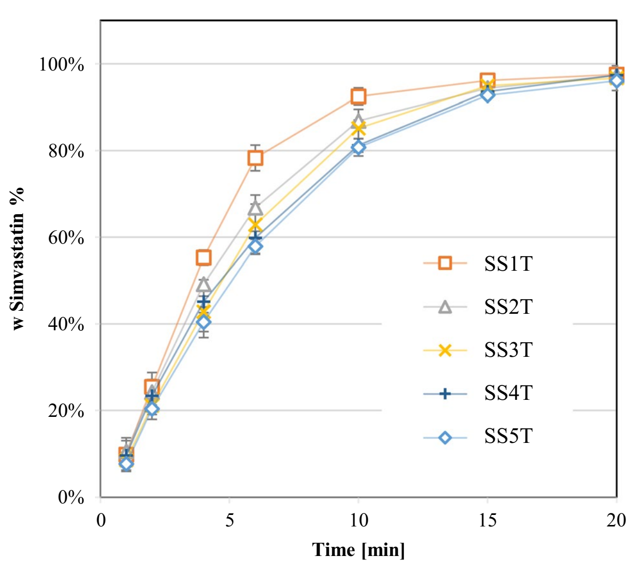

Fig. 13 USP2 paddle dissolution profiles of tablets prepared from granulates of different densification (from 50 to 250 MPa) – SS1T (Square); SS2T (Triangle); SS3T (Cross); SS4T (Plus); SS5T (Rhombus)

Conclusion

In this study, the effects of roller compaction on the dissolution behaviours of granules and tablets for two pharmaceutical formulations, containing Dapagliflozin (BCS3) and Simvastatin (BCS2), were thoroughly investigated. The results demonstrate the role of compaction parameters and particle characteristics in influencing dissolution performance. For Dapagliflozin, a well-soluble API, the densification of granules had minimal impact on the dissolution and the dissolution profiles were consistent for both granules and tablets. When studying the Simvastatin formulation, containing a poorly soluble API, it was revealed that there is a dependency on compaction pressure and granule size. Higher compaction pressures resulted in slower release, particularly for larger granule size fractions. The dissolution testing of granules served as an effective early-stage predictor of tablet performance. It reveals the importance of optimizing granulation parameters, including sieving and granule size distribution, to balance dissolution and other engineering properties, such as flow properties. When the results between granules and tablet dissolution are both considered, there is merit to both of these testing procedures. Granules dissolution testing uncovered a broader understanding of dissolution behaviour early on. The comparative analysis of USP4 and USP2 dissolution methods suggests that early granule dissolution studies are useful for process optimization. USP4 provided detailed and discriminatory profiles, easing the identification of potential formulation challenges at an earlier stage. These findings suggest that granule dissolution testing can significantly reduce the reliance on extensive tablet-level testing, ultimately accelerating the development cycle and improving resource efficiency. While this study utilized specific formulations for Dapagliflozin and Simvastatin, the observed dependence on API solubility aligns with general principles of dissolution for BCS Class II and III compounds. However, the extent to which compaction affects dissolution can also be influenced by excipient properties (e.g., deformability, disintegration potential), which were not varied here. Further studies with different excipient combinations would be beneficial to confirm the broader applicability of using granule dissolution as an early predictor across different dry granulation formulations.

If necessary to achieve a more insightful and generalized relationship between roller compaction and granule dissolution, employing a more discriminating design of experiments (DoE) would be relevant.

Acknowledgements The authors acknowledge academic support from the University of Chemistry and Technology in Prague (UCT Prague) and The Pharmaceutical Applied Research Centre (The PARC), as well as industrial support from Zentiva k.s. in Prague, Czech Republic.

Authors Contribution Nikita Marinko: Conceptualization, Investigation, Data Curation, Methodology, Validation, Visualization, Writing – original draft, Writing – Review and Editing. Vít Zvoníček: Conceptualization, Supervision. Petr Zámostný: Conceptualization, Methodology, Validation, Writing – Review and Editing, Supervision. Stephanie Michelle Medrano: Formal Analysis, Visualization, Methodology. Tomáš Krpelan: Formal Analysis. Zuzana Chayka: Formal Analysis, Methodology. Kateřina Budková: Formal Analysis.

Funding Open access publishing supported by the institutions participating in the CzechELib Transformative Agreement. The authors gratefully acknowledge financial support from Specific University Research projects A2_FCHT_2023_087 and A2_FCHT_2024_009.

Data Availability The data that support the findings of this study are available from the first author upon reasonable request.

Declarations

Competing interests The authors declare that they have no known competing financial interests or personal relationships that could have appeared to influence the work reported in this paper.

References

1. Smrčka D, Dohnal J, Štěpánek F. Dissolution and disintegration kinetics of high-active pharmaceutical granules produced at laboratory and manufacturing scale. Eur J Pharm Biopharm. 2016;106:107–16. https://doi.org/10.1016/j.ejpb.2016.04.005.
2. Sauer A, et al. Downstream processing of spray-dried ASD with hypromellose acetate succinate – roller compaction and subsequent compression into high ASD load tablets. Int J Pharm: X. 2021;3:100099. https://doi.org/10.1016/j.ijpx.2021.100099.
3. Kuentz M, Holm R, Elder DP. Methodology of oral formulation selection in the pharmaceutical industry. Eur J Pharm Sci. 2016;87:136–63. https://doi.org/10.1016/j.ejps.2015.12.008.
4. Sun C, Himmelspach MW. Reduced tabletability of roller compacted granules as a result of granule size enlargement. J Pharm Sci. 2006;95(1):200–6. https://doi.org/10.1002/jps.20531.
5. Wilms A, Kleinebudde P. Towards better understanding of the influence of process parameters in roll compaction/dry granulation on throughput, ribbon microhardness and granule failure load. Int J Pharm: X. 2020;2:100059. https://doi.org/10.1016/j.ijpx.2020.100059.
6. Muthancheri I, et al. Modified roller compaction model to account for roll speed effect on powder compaction in dry granulation process. J Pharm Sci. 2024;113(8):2484–91. https://doi.org/10.1016/j.xphs.2024.05.006.
7. Wilson D, Wren S, Reynolds G. Linking dissolution to disintegration in immediate release tablets using image analysis and a population balance modelling approach. Pharm Res. 2012;29(1):198–208. https://doi.org/10.1007/s11095-011-0535-1.
8. Leane M, Pitt K, Reynolds G. A proposal for a drug product manufacturing classification system (MCS) for oral solid dosage forms. Pharm Dev Technol. 2015;20(1):12–21. https://doi.org/10.3109/10837450.2014.954728.
9. Palugan L, et al. Dry granulation by roller compaction of paracetamol with different grades of mannitol. J Drug Deliv Sci Technol. 2025;106: 106689. https://doi.org/10.1016/j.jddst.2025.106689.
10. Yu S, et al. The effects of lubrication on roll compaction, ribbon milling and tableting. Chem Eng Sci. 2013;86:9–18. https://doi.org/10.1016/j.ces.2012.02.026.
11. Sacher S, Khinast J. An overview of pharmaceutical manufacturing for solid dosage forms. Methods Pharmacol Toxicol. 2015;32:311–83. https://doi.org/10.1007/978-1-4939-2996-2_10.
12. Kazemi P, et al. Effect of roll compaction on granule size distribution of microcrystalline cellulose-mannitol mixtures: computational intelligence modeling and parametric analysis. Drug Des Devel Ther. 2017;11:241–51. https://doi.org/10.2147/dddt.S124670.
13. Patel S, et al. Understanding size enlargement and hardening of granules on tabletability of unlubricated granules prepared by dry granulation. J Pharm Sci. 2011;100(2):758–66. https://doi.org/10.1002/jps.22315.
14. Kašpar O, et al. Combined UV/vis and micro-tomography investigation of acetaminophen dissolution from granules. Int J Pharm. 2013;458(2):272–81. https://doi.org/10.1016/j.ijpharm.2013.10.032.
15. Gabbott I. Designer granules : beating the trade-off between granule strength and dissolution time. Doctoral Thesis, University of Sheffield; 2007. https://etheses.whiterose.ac.uk/3605/.
16. Arndt O-R, et al. Impact of different dry and wet granulation techniques on granule and tablet properties: a comparative study. J Pharm Sci. 2018;107(12):3143–52. https://doi.org/10.1016/j.xphs.2018.09.006.
17 Shanmugam S. Granulation techniques and technologies: recent progresses. BioImpacts : BI. 2015;5(1):55–63. https://doi.org/10.15171/bi.2015.04.
18. Gamble J, et al. Roller compaction: application of an in-gap ribbon porosity calculation for the optimization of downstream granule flow and compactability characteristics. Pharm Dev Technol. 2010;15:223–9. https://doi.org/10.3109/10837450903095342.
19. Inghelbrecht S, Remon JP. Reducing dust and improving granule and tablet quality in the roller compaction process. Int J Pharm. 1998;171(2):195–206. https://doi.org/10.1016/S0378-5173(98)00195-1.
20. Kamata T, Wada K, Ichikawa H. Dry pre-coating of active pharmaceutical ingredient with submicron-sized hydroxypropylcellulose in dry granulation using roller compactor improves granule properties. J Drug Deliv Sci Technol. 2018;43:34–43. https://doi.org/10.1016/j.jddst.2017.08.009.

21. Falzone AM, Peck GE, Mccabe GP. Effects of changes in roller compactor parameters on granulations produced by compaction. Drug Dev Ind Pharm. 1992;18(4):469–89. https://doi.org/10.3109/03639049209043864.
22. Souihi N, et al. Design space estimation of the roller compaction process. Ind Eng Chem Res. 2013;52(35):12408–19. https://doi.org/10.1021/ie303580y.
23. Matji A, et al. Predicting the critical quality attributes of ibuprofen tablets via modelling of process parameters for roller compaction and tableting. Int J Pharm. 2019;565:209–18. https://doi.org/10.1016/j.ijpharm.2019.05.011.
24. Chang CK, et al. Roller compaction, granulation and capsule product dissolution of drug formulations containing a lactose or mannitol filler, starch, and talc. AAPS PharmSciTech. 2008;9(2):597–604. https://doi.org/10.1208/s12249-008-9088-y.
25. Inghelbrecht S, Remon JP. Roller compaction and tableting of microcrystalline cellulose/drug mixtures. Int J Pharm. 1998;161:215–24. https://doi.org/10.1016/S0378-5173(97)00356-6.
26. Dular Vovko A, et al. Influence of formulation factors, process parameters, and selected quality attributes on carvedilol release from roller-compacted hypromellose-based matrix tablets. Pharmaceutics. 2022. https://doi.org/10.3390/pharmaceutics14040876.
27. Anuschek M, et al. Terahertz time-domain spectroscopy for the investigation of tablets prepared from roller compacted granules. Int J Pharm. 2023;642: 123165. https://doi.org/10.1016/j.ijpharm.2023.123165.
28. Hwang KM, et al. Use of roller compaction and fines recycling process in the preparation of erlotinib hydrochloride tablets. Eur J Pharm Sci. 2019;131:99–110. https://doi.org/10.1016/j.ejps.2019.01.036.
29. Matsunami K, et al. Surrogate modeling of dissolution behavior toward efficient design of tablet manufacturing processes. Comput Chem Eng. 2023. https://doi.org/10.1016/j.compchemeng.2023.108141.
30. Kim JY, Chun MH, Choi DH. Control strategy for process development of high-shear wet granulation and roller compaction to prepare a combination drug using integrated quality by design. Pharmaceutics. 2021. https://doi.org/10.3390/pharmaceutics13010080.
31. Mitchell SA, Reynolds TD, Dasbach TP. A compaction process to enhance dissolution of poorly water-soluble drugs using hydroxypropyl methylcellulose. Int J Pharm. 2003;250(1):3–11. https://doi.org/10.1016/S0378-5173(02)00293-4.
32. Rajkumar AD, et al. The effect of roller compaction and tableting stresses on pharmaceutical tablet performance. Powder Technol. 2019;341:23–37. https://doi.org/10.1016/j.powtec.2018.08.065.
33. Vanova N, et al. Effect of process scale-up on granulate, tablets properties and dissolution behavior in immediate release fixed-dose combination product. Maced Pharm Bull. 2020;66:137–8. https://doi.org/10.33320/maced.pharm.bull.2020.66.03.068.
34. Ye X, et al. Effects of processing on a sustained release formulation prepared by twin-screw dry granulation. J Pharm Sci. 2019;108(9):2895–904. https://doi.org/10.1016/j.xphs.2019.04.004.
35. Murakami H, et al. Correlation between loose density and compactibility of granules prepared by various granulation methods. Int J Pharm. 2001;216(1):159–64. https://doi.org/10.1016/S0378-5173(01)00575-0.
36. Galata DL, et al. Applications of machine vision in pharmaceutical technology: a review. Eur J Pharm Sci. 2021;159: 105717. https://doi.org/10.1016/j.ejps.2021.105717.
37. Kader, M. Mitigating the risks of generic drug product development: an application of quality by design (QbD) and question based review (QbR) approaches. J Excip Food Chem 2016;7:35–75. Available from: https://www.semanticscholar.org/paper/Mitigating-the-Risks-of-Generic-Drug-Product-An-of-Kader/d9597bce3d9772bac1084c79437ffa1546021d5b.
38. Dutt H, Joshi M, Burade N. Roller compaction process: components, mathematical modelling and recent PAT tools. Int J Pharm Pharm Res. 2020; https://ijppr.humanjournals.com/wpcontent/uploads/2020/09/43.Himanshu-Dutt-Mahendra-Joshi-Nikhil-Burade.pdf.
39. Yamashita H, Sun CC. Material-sparing and expedited development of a tablet formulation of carbamazepine glutaric acid cocrystal- a QbD approach. Pharm Res. 2020;37(8):153. https://doi.org/10.1007/s11095-020-02855-3.
40. Lopes MIQCD. In vitro and in silico dissolution and permeation assessment. In: Mestre em Engenharia Química e Bioquímica. Universidade Nova de Lisboa; 2017. http://hdl.handle.net/10362/99428.
41. Soh JLP, Heng PWS. In vitro dissolution of pharmaceutical solids. Oral Bioavailability. 2011:39–49. https://doi.org/10.1002/9781118067598.ch4.
42. Wiser L, et al. Solubility of pharmaceutical solids. Oral Bioavailability. 2011:21–38. https://doi.org/10.1002/9781118067598.ch3.
43. Marinko N, Zámostný P. Meloxicam carrier systems having enhanced release and aqueous wettability prepared using microsuspensions in different liquid media. AAPS PharmSciTech. 2020;21(5):155. https://doi.org/10.1208/s12249-020-01701-4.
44. Zámostný P, et al. Drug release from carrier systems comprising meloxicam crystals formed by impregnation-evaporation. Crystals. 2023;13(3):527. https://doi.org/10.3390/cryst13030527.
45. Khan KA, Rhodes CT. Effect of variation in compaction force on properties of six direct compression tablet formulations. J Pharm Sci. 1976;65(12):1835–7. https://doi.org/10.1002/jps.2600651235.
46. Patel S, Kaushal AM, Bansal AK. Compression physics in the formulation development of tablets. Crit Rev Ther Drug Carrier Syst. 2006;23(1):1–65. https://doi.org/10.1615/critrevtherdrugcarriersyst.v23.i1.10.
47. Evelghem JV. Improving tablet quality with compression to equal force technology. Pharm Technol. 2008. Available from: https://www.pharmtech.com/view/improving-tablet-quality-compression-equal-forcetechnology.
48. Reynolds G. Model-based development of roller compaction processes; 2019. p. 119–45. https://doi.org/10.1002/9781119600800.ch55.
49. Reynolds G, et al. Practical application of roller compaction process modeling. Comput Chem Eng. 2010;34(7):1049–57. https://doi.org/10.1016/j.compchemeng.2010.03.004.
50. Johanson JR. A rolling theory for granular solids. J Appl Mech. 1965;32(4):842–8. https://doi.org/10.1115/1.3627325.
51. Marinko N, et al. Method to determine envelope density for roller compacted ribbons by solid displacement of glass microspheres. Powder Technol. 2024;444: 120014. https://doi.org/10.1016/j.powtec.2024.120014.
52. Singla N, et al. A discriminatory and biorelevant dissolution test method for Simvastatin drug products. Dissolution Technol. 2009;16:11–3. https://doi.org/10.14227/DT160409P11.
53. Zámostny, P et al. Mechanisms of tabled disintegration and drug release - towards the deeper understanding of the dissolution process. In: 9th international conference on chemical technology (ICCT). 2022. Available from: WOS:001242890900051.
54. Dehont FR, et al. Briquetting and granulation by compaction new granulator-compactor for the pharmaceutical industry. Drug Dev Ind Pharm. 1989;15(14–16):2245–63. https://doi.org/10.3109/03639048909052530.
55. Hattori Y, Ariyasu A, Otsuka M. Delay effect of magnesium stearate on tablet dissolution in acidic medium. Int J Pharm. 2016;511(2):757–64. https://doi.org/10.1016/j.ijpharm.2016.07.034.

56. Uzunović A, Vranić E. Effect of magnesium stearate concentration on dissolution properties of ranitidine hydrochloride coated tablets. Bosn J Basic Med Sci. 2007;7(3):279–83. https://doi.org/10.17305/BJBMS.2007.3060.
57. Reimer HL, Kleinebudde P. Hybrid modeling of roll compaction processes with the Styl'one evolution. Powder Technol. 2019;341:66–74. https://doi.org/10.1016/j.powtec.2018.02.052.
58. Peter S, Lammens RF, Steffens K-J. Roller compaction/dry granulation: use of the thin layer model for predicting densities and forces during roller compaction. Powder Technol. 2010;199(2):165–75. https://doi.org/10.1016/j.powtec.2010.01.002.
59. Patel BA, et al. Predicting the pressure distribution during roll compaction from uniaxial compaction measurements. Chem Eng J. 2010;164(2):410–7. https://doi.org/10.1016/j.cej.2009.12.022.
60. Zinchuk AV, Mullarney MP, Hancock BC. Simulation of roller compaction using a laboratory scale compaction simulator. Int J Pharm. 2004;269(2):403–15. https://doi.org/10.1016/j.ijpharm.2003.09.034.
61. Märkle N, Warnke G, Pein-Hackelbusch M. An iterative process and mixture design approach for dry granulated ternary blends of filler-binders. Int J Pharm: X. 2025. https://doi.org/10.1016/j.ijpx.2025.100331.
62. Palugan L, et al. Evaluation of different types of mannitol for dry granulation by roller compaction. SSRN Electron J. 2022. https://doi.org/10.2139/ssrn.4120267.
63. Chendo C, Pinto J, Paisana M. Comprehensive powder flow characterization with reduced testing. Int J Pharm. 2023. https://doi.org/10.1016/j.ijpharm.2023.123107.
64. Goh HP, Heng P, Liew C. Comparative evaluation of powder flow parameters with reference to particle size and shape. Int J Pharm. 2018;547:133. https://doi.org/10.1016/j.ijpharm.2018.05.059.
65. Shi H, et al. Effect of particle size and cohesion on powder yielding and flow. Kona Powder Part J. 2018;35:226–50. https://doi.org/10.14356/KONA.2018014.
66. Capece M, et al. On the relationship of inter-particle cohesiveness and bulk powder behavior: flowability of pharmaceutical powders. Int J Pharm. 2016;511(1):178–89. https://doi.org/10.1016/j.ijpharm.2016.06.059.
67. Ban S, Goodwin D. The impact of granule density on tableting and pharmaceutical product performance. Pharm Res. 2017;34:1002–11. https://doi.org/10.1007/s11095-017-2115-5.
68. Rajkumar A, et al. Investigating the effect of processing parameters on pharmaceutical tablet disintegration using a real-time particle imaging approach. Eur J Pharm Biopharm. 2016;106:88–96. https://doi.org/10.1016/j.ejpb.2016.06.005.
69. Perez-Gandarillas L, et al. Effect of roll-compaction and milling conditions on granules and tablet properties. Eur J Pharm Biopharm. 2016;106:38–49. https://doi.org/10.1016/j.ejpb.2016.05.020.
70. Monteyne T, et al. Continuous melt granulation: influence of process and formulation parameters upon granule and tablet properties. Eur J Pharm Biopharm. 2016;107:249–62. https://doi.org/10.1016/j.ejpb.2016.07.021.
71. Maniruzzaman M, et al. A quality by design (QbD) twin-screw extrusion wet granulation approach for processing water insoluble drugs. Int J Pharm. 2017;526(1–2):496–505. https://doi.org/10.1016/j.ijpharm.2017.05.020.
72. Ansari MA, Stepanek F. The effect of granule microstructure on dissolution rate. Powder Technol. 2008;181(2):104–14. https://doi.org/10.1016/j.powtec.2006.12.012.
73. Smrčka D, Dohnal J, Štěpánek F. Effect of process scale-up on the dissolution of granules with a high content of active pharmaceutical ingredient. Powder Technol. 2015;285:88–95. https://doi.org/10.1016/j.powtec.2015.04.028.